

# Dipole Source Reconstruction By Convolutional Neural Networks

Jiayi He<sup>1</sup>, Qiaolei Huang<sup>1</sup>, Jun Fan<sup>1</sup>

<sup>1</sup>*Electromagnetic Compatibility Laboratory, Missouri University of S&T, Rolla, MO, USA*  
hejiay, qh5x4, and jfan@mst.edu

**Abstract**—Equivalent dipole moments are widely used for noise source reconstruction in radio frequency interference (RFI) study. The equivalent dipole sources are usually extracted from measured near-field pattern. This paper introduces a machine learning based method to extract the dipole moments. A convolutional neural network is trained to perform a multi-label classification to determine the type of dipole moments. The locations of the dipole moments are obtained from the global averaging pooling layer. Then the magnitude and phase of the dipoles can be calculated from least square (LSQ) optimization. The proposed method is tested on simulated near-field patterns. The comparison between reconstructed field pattern and original field pattern is given.

**Keywords**—radio frequency interference (RFI), dipole moment, machine learning, convolutional neural network (CNN)

## I. INTRODUCTION

As the data rate in electronic devices gets higher, radio frequency interference (RFI) problems are becoming more significant. In the study of RFI problems, equivalent dipole moments are widely used to reconstruct the noise source [1]-[4]. The coupled voltage or coupled power can be calculated from the reconstructed dipole sources. Designers can also improve the design to mitigate the coupling based on the equivalent source models.

Since dipole sources reconstruction can help the analysis and design significantly, various methods have been developed to extract dipole moments. With a uniform array of electric and magnetic dipole moments predefined, the least square (LSQ) method can be used to solve the magnitude and phase of each dipole moment [4]. However, this method is sensitive to measurement noise and the solution may be non-physical when the size of the dipole array gets large. Optimization methods such as Genetic algorithm are also common solutions to this problem [5], [6]. But the convergence and computation time of optimization methods usually depend on the initial value. A machine learning method based on support vector machine (SVM) have been used to classify the dominant dipole type from the image of the near-field pattern [7]. The location of the dipole is further determined from auto-correlation calculation after the type is identified. This method shows the capability of pattern recognition techniques in field pattern classification and dipole source reconstruction.

This paper proposes a machine learning based dipole source reconstruction method using convolutional neural networks

(CNN). CNNs are widely used to process 2-D grid data such as images. CNNs have also been used to solve electromagnetic problems [8]. The picture of the electromagnetic field is fed to the convolutional neural network, and the CNN performs a multi-label classification to determine all types of dominant dipole moments. The CNN also generates a class activation map, which indicates the locations of each type of present dipole moment [9]. With the types and locations of the dipoles known, the magnitude and phase of each dipole can be obtained from LSQ or other optimization methods.

This paper is organized as follows. In Section II, the algorithm of extracting the type and location of dipole sources from a near-field pattern is illustrated. In Section III, the proposed method is validated with several simulated test cases. Section IV concludes the paper finally.

## II. MACHINE LEARNING BASED DIPOLE RECONSTRUCTION

Dipole moments are the most basic radiation sources. An infinitely small electrical current segment forms an electrical dipole. An infinitely small current loop forms a magnetic dipole. The electrical dipole is denoted as a P dipole and the magnetic dipole is denoted as an M dipole. There are six types of basic dipole moments based on the orientations as shown in Fig. 1. The near field of each basic dipole moment can be calculated from analytical formulas. Each basic dipole moment also has its unique near field patterns. The feature of the pattern can be used to classify the type of the dipole moment by machine learning algorithms.

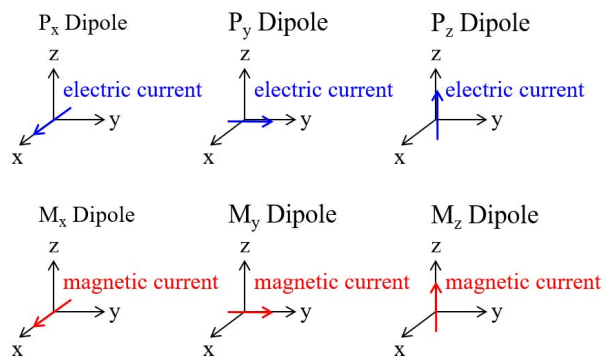


Fig.1. Six types of basic dipole moments

#### A. Convolution Neural Network for Multi-Label Classification

In machine learning and computer vision, the convolutional neural network is a typical neural network used for image classification analysis [10]. In this work, a set of field pattern pictures generated from analytical formulas is given as the training dataset. Each picture is labeled with the categories of the present dipoles. If a type of dipole moment exists in the field pattern, this category is labeled with 1, otherwise it is labeled with 0. As a result, the label for each picture is a 1 by 6 array and each element in the array is either 1 or 0. In convolutional neural networks, there are usually a few convolutional layers with rectified linear unit (ReLU) function as the activation function and pooling layers. Since it's possible that multiple types of dipole moments are present, different types of dipole moments are not exclusive and a multi-label classification task is desired. Therefore, the activation function of the last layer is the sigmoid function instead of the softmax function, which is widely used as the activation function in multi-class classification tasks. The sigmoid function is shown as follows:

$$\text{sigmoid}(x) = \frac{1}{1 + e^{-x}} \quad (1)$$

The output of the sigmoid function can be interpreted as the probability of the input belonging to this category. The loss function is the cross entropy between the output logits and the corresponding labels as shown in (2),

$$\text{cross\_entropy} = -z \times \log(\text{sigmoid}(\alpha)) - (1-z) \times \log(1 - \text{sigmoid}(\alpha)) \quad (2)$$

where  $z$  is the label vector of the picture and  $\alpha$  is the output of the neural network before the sigmoid activation function. With the sigmoid cross entropy as the loss function, the convolutional neural network is supposed to recognize all the present types of dipoles in the given field pattern.

#### B. Class Activation Map

To get the location of each type of dipole, the class activation mapping (CAM) technique is used. In image processing, a class activation map for a particular category indicates the discriminative image regions used by the CNN to identify that category. CAM can be generated using global averaging pooling after the last convolutional layer. Global averaging pooling outputs the spatial average of the feature map at the last convolutional layer. Then a fully-connected layer is used as the last layer to produce the final output.

For a given image, let  $f_k(x, y)$  represent the output of unit  $k$  in the last convolutional layer at location  $(x, y)$ . Then equation (3) shows the result of global average pooling.

$$F^k = \sum_{x,y} f_k(x, y) \quad (3)$$

The final score of a given class  $c$ ,  $S_c$ , is calculated in (4).

$$S_c = \sum_k \omega_k^c F_k \quad (4)$$

where  $\omega_k^c$  is the weight corresponding to class  $c$  for unit  $k$  in the last fully-connected layer. By plugging equation (3) into (4), the final score can be expressed in (5).

$$\begin{aligned} S_c &= \sum_k \omega_k^c \sum_{x,y} f_k(x, y) \\ &= \sum_{x,y} \sum_k \omega_k^c f_k(x, y) \end{aligned} \quad (5)$$

Then the class activation map for class  $c$ , denoted as  $M_c$ , is defined in (6).

$$M_c(x, y) = \sum_k \omega_k^c f_k(x, y) \quad (6)$$

Since the total score is the spatial summation of the class activation map, the class activation map directly indicates the importance of the image region leading to a certain class. The image region with larger values in the class activation map tends to be more relevant to this class. In this work, if a certain type of dipole moment is recognized by the neural network, the class activation map is calculated to identify the location of this dipole moment.

#### C. Dipole Extraction Algorithm by CNN

The structure of the CNN is shown in Fig. 2. The batch size is 256 in this structure. After the input layer, there are two 2D convolutional layers connecting in series to increase the network complexity and function-fitting ability. Then a linear layer is used to reduce the dimension of the data. Finally a fully-connected layer with sigmoid activation function is used to generate the classification outputs. The last fully-connected layer is also used to compute the class activation map.

3000 field patterns generated from analytical formulas and their corresponding labels are used as training data. A learning rate of 0.01 with Adam Optimizer is used in training. The loss on test data is shown in Fig. 3. The loss converges after 40 epochs.

The workflow of the proposed dipole source reconstruction is shown in Fig. 4. First the unknown field pattern is fed to the trained convolutional neural network to determine the types of dipole moments in this pattern. For each type of the dipole moment that is identified, the corresponding class activation map is calculated to determine its location.

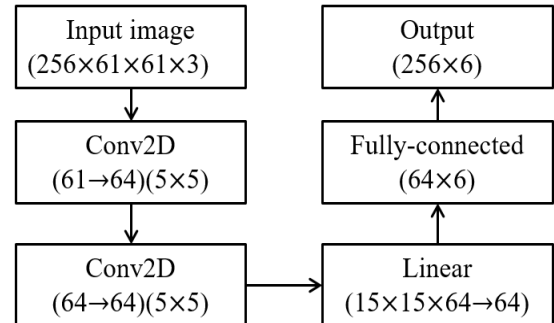


Fig.2. The structure of the CNN layer

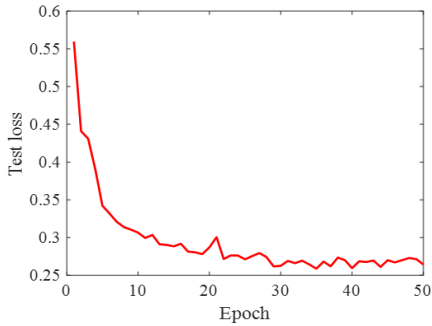


Fig. 3. Testing loss graph of the neural network

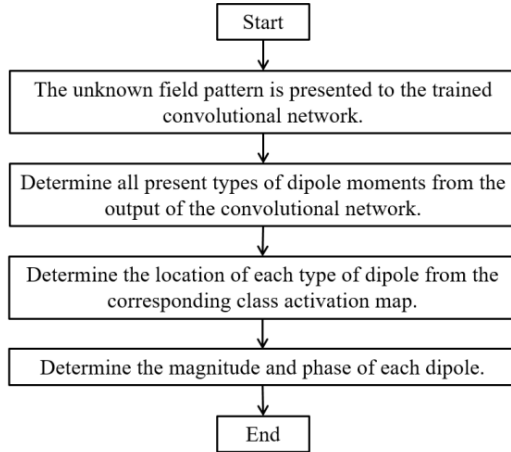


Fig.4. Workflow of the proposed algorithm

### III. VALIDATION

Several simulation examples are discussed below to validate the proposed method. The field pattern of the first example is shown in Fig.5. This pattern is from a simple  $M_x$  dipole and used to illustrate the function of class activation map. The neural network classifies the field pattern to  $M_x$  dipole category. Then the class activation map for this category is calculated and the result is shown in Fig. 6.

In the class activation map, the hot region represents the location that is most relevant to this category, thus indicating the location of the dipole moment. It can be seen that the region with largest color value in fig. 6 corresponds to the location of the dipole in the field pattern shown in Fig. 5. Though the location information are not provided and only image-level labels are

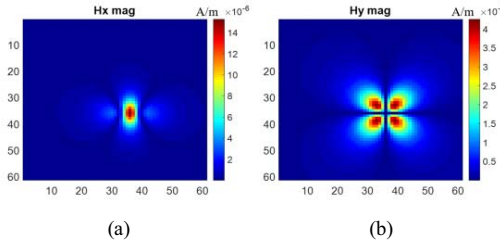


Fig.5. Field patterns of the input image in example 1. (a).  $H_x$ . (b).  $H_y$ .

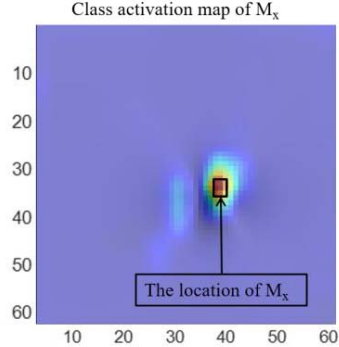


Fig.6. Class activation map of the  $M_x$  dipole type

used in the training, this algorithm has the ability to locate the feature of a certain category.

The  $H_x$  and  $H_y$  field patterns of the second example are shown in Fig. 7. The field pattern picture is sent to the pre-trained convolutional neural network. Two types of dipoles,  $M_x$  and  $M_z$ , are identified by the network. Similarly, the class activation maps for these two categories are calculated and the results are shown in Fig. 8.

In the class activation map for  $M_x$  dipole, it is clear that there is only one red region and the location of the largest value in this map is the location of the  $M_x$  dipole. The location of the  $M_z$  dipole is also where the largest value locates in the  $M_z$  dipole map. The map for  $M_z$  dipole is noisier than the map for  $M_x$  in this example. Possible reasons can be the imbalance of the training data or hyper-parameters not being well-tuned. With the types and the locations of the dipoles known, their magnitudes and phases can be determined by least square or optimization

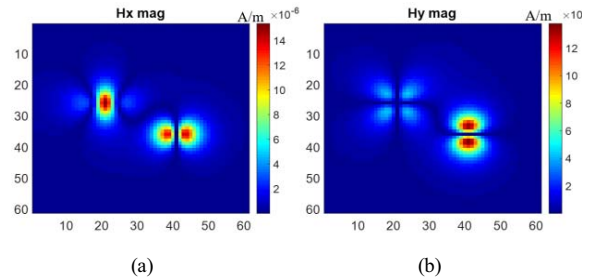


Fig. 7. Field patterns of the input image in example 2. (a).  $H_x$ . (b).  $H_y$ .

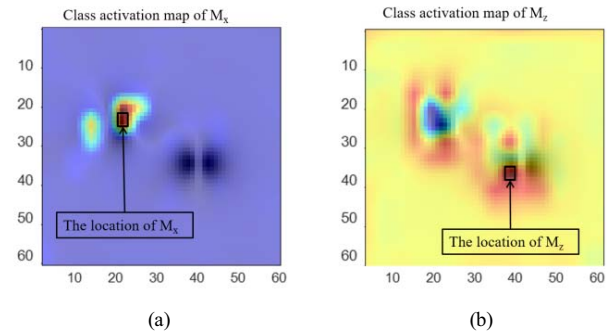


Fig. 8. The class activation maps of (a).  $M_x$ . (b).  $M_z$

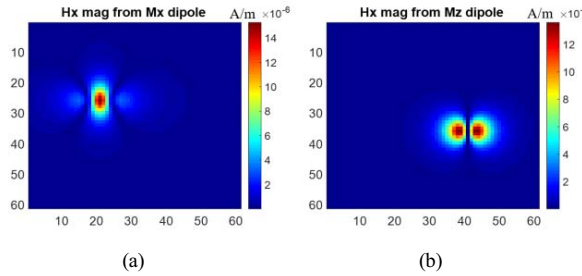


Fig. 9.  $H_x$  patterns from the extracted dipoles. (a).  $M_x$ . (b).  $M_z$

methods. The  $H$  fields from the  $M_x$  dipole moment and the  $M_z$  dipole moment at the detected locations are shown in Fig. 9.

Since two dipoles are located far away from each other, the field pattern in Fig. 7 is relatively easier to recognize. A more complex example is tested on the proposed algorithm. The field pattern is shown in Fig. 10.

In this example, the probability for  $M_x$  and  $M_y$  categories is more than 99% and 20% for  $M_z$  from the neural network output. For other categories, the probability is less than 1%. If 50% is used as the threshold,  $M_x$  and  $M_y$  are two types of dipole moments identified by the algorithm. Their corresponding class activation maps are shown in Fig. 11. It can be observed that the  $M_x$  and  $M_y$  dipoles are pretty close to each other. Similarly, the magnitudes and phases of the dipoles can be further determined. The  $H$  fields from the  $M_x$  dipole moment and the  $M_y$  dipole moment at the detected locations are shown in Fig. 12. The reconstructed field is compared to the original field as shown in Fig. 13. It can be seen that the reconstructed field pattern is very close to the input pattern.

The main advantage of the proposed algorithm is that it can determine the dipole moment types and their corresponding

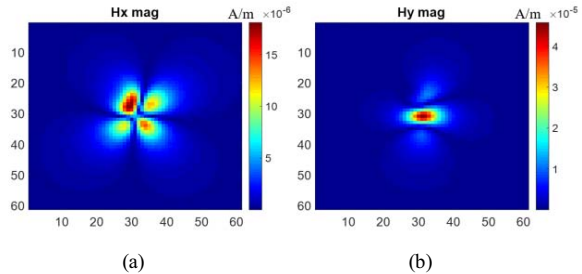


Fig. 10. Field patterns of the input image in example 3. (a).  $H_x$ . (b).  $H_y$ .

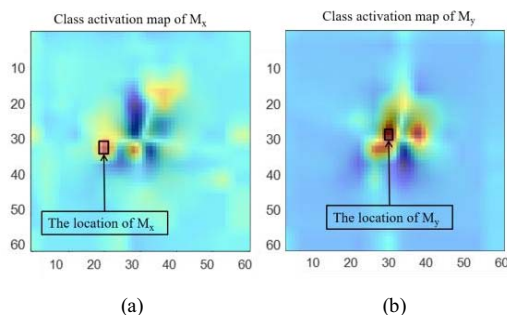


Fig. 11. The class activation maps of (a).  $M_x$ . (b).  $M_y$ .

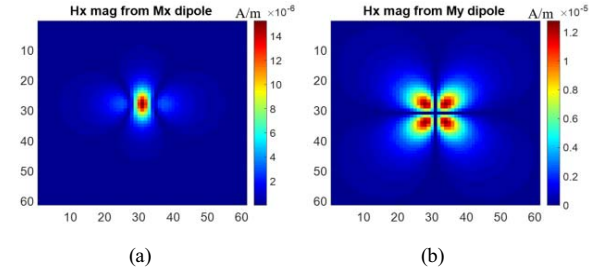


Fig. 12.  $H_x$  patterns from the extracted dipoles. (a).  $M_x$ . (b).  $M_y$

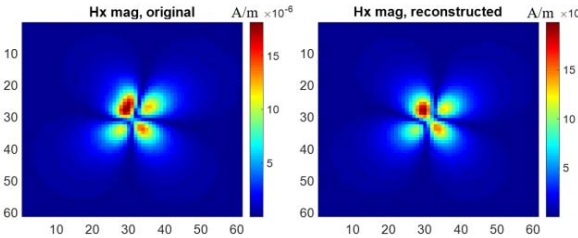


Fig. 13. The structure of the CNN layer

locations in a short time with a well-trained neural network. Then the calculation of the magnitude and phase of each dipole with the location and type known is much easier than directly performing an optimization algorithm to extract dipole sources. The main drawback of this method is its generalization capability, like other machine learning based algorithms, is affected by the quality of training data and the values of hyper-parameters. Data augmentations and hyper-parameters tunings are needed to further improve the algorithm.

#### IV. CONCLUSION

This paper proposes a machine learning based dipole source reconstruction method. A multi-label classification analysis is performed by a convolutional neural network to determine the types of the dipole moment sources. This algorithm further uses the class activation map technique to determine the location of the dipoles. Three simulation examples are presented to validate the proposed algorithm and show how the class activation map can help locate the dipoles. Future work includes testing the proposed algorithm on measured field patterns and improving this algorithm by doing data augmentations and tuning hyper-parameters.

#### REFERENCES

- [1] Q. Huang, F. Zhang, T. Enomoto, J. Maeshima, K. Araki and C. Hwang, "Physics-based dipole moment source reconstruction for RFI on a practical cellphone", *IEEE Trans. Electromagn. Compat.*, vol. 59, no. 6, pp. 1693-1700, Dec. 2017.
- [2] C. Hwang and Q. Huang, "IC placement optimization for RF interference based on dipole moment sources and reciprocity," *IEEE Asia-Pacific Electromagn. Compat. Symp.*, 2017, pp.331-333.
- [3] Q. Huang, Y. Liu, L. Li, Y. Wang, C. Wu and J. Fan, "Radio Frequency Interference Estimation Using Transfer Function Based Dipole Moment Model," *IEEE Asia-Pacific Electromagn. Compat. Symp.*, 2018, pp.115-120.

- [4] Z. Yu, J. A. Mix, S. Sajuyigbe, K. P. Slattery, and J. Fan, "An improved dipole-moment model based on near-field scanning for characterizing near-field coupling and far-field radiation from an IC," *IEEE Trans. Electromagn.*
- [5] J. Zhang and J. Fan, "Source reconstruction for IC radiated emissions based on magnitude-only near-field scanning," *IEEE Trans. Electromagn.*
- [6] C. Wu, Z. Sun, Q. Huang, Y. Wang, J. Fan, J. Zhou, "A Method to Extract Physical Dipoles for Radiating Source Characterization and Near Field Coupling Estimation", in Proc. of IEEE Int. Symp. Electromagn.Compat., 2019, pp. 580-583
- [7] Q. Huang and J. Fan, "Machine Learning Based Source Reconstruction for RF Desense", *IEEE Trans. Electromagn. Compat.*, vol. 60, no. 6, pp. 1640-1647, Dec. 2018.
- [8] L. Zhang et al., "Decoupling Capacitor Selection Algorithm for PDN Based on Deep Reinforcement Learning," 2019 IEEE International Symposium on Electromagnetic Compatibility, Signal & Power Integrity (EMC+SIPI), New Orleans, LA, USA, 2019, pp. 616-620.
- [9] B. Zhou, A. Khosla, A. Lapedriza, A. Oliva, and A. Torralba, "Learning deep features for discriminative localization," in *Proceedings of the IEEE conference on computer vision and pattern recognition*, 2016, pp. 2921-2929.
- [10] I. Goodfellow, Y. Bengio, and A. Courville, *Deep Learning*. Cambridge, MA, USA: MIT Press, 2016. [Online]. Available: <http://www.deeplearningbook.org>